High-Performance Cascaded Surface-Illuminated Ge-on-Si APD Array

XiaoBin Liu, XueTong Li, YingZhi Li, ZiHao ZHi, BaiSong Chen, HeMing Hu, QiJie Xie, QuanXin Na, XueYan Li, PengFei Guo, FengLi Gao, GuoQiang Lo, BoNan Kang, and JunFeng Song

***Abstract*— In this letter, we report a cascaded surface-illuminated Germanium-on-Silicon (Ge-on-Si) avalanche photodiode (APD) array with a low dark current. The photodetector array cascades seven Ge-on-Si APDs through interconnecting the charge regions to form photomultiplier tubesiPMTjC which increases the effective light absorption area compared to the single APD scheme. To the best of our knowledge, this is the first time that Ge-on-Si PMT has been reported. The optimum response of single-electrode (2 pixels) Ge-on-Si APD is 2.4 A/W with a dark current of 100 nA, and the optimum bandwidth is 52 MHz. PMT has a responsivity of approximately 3 times that of a single-electrode Ge-on-Si APD for the same dark current (100 nA). With low dark current, our PMT has a better optical amplification effect than the parallel Ge-on-Si PD. We have also further tested the current tuning properties of the Ge-on-Si APD arrays with different applied Ge voltages. The test demonstrates the feasibility of cascading three-electrode APD arrays. A cascaded Ge-on-Si APD array with good photodetection properties at low-light conditions has been demonstrated which provides guidance for the design of large-scale Ge-on-Si APD arrays for light detection and ranging application.**

***Index Terms*— Ge-on-Si APD, PMT, low dark current, low-light detection, photodetector array.**

I. Introduction

IN LIGHT detection and ranging (LiDAR) systems for autonomous driving, photodetectors with large effective detection areas are required to improve the detection accuracy and efficiency. The current photodetector arrays are mainly III-V material based avalanche photodetector (APD) arrays and silicon (Si) CMOS device arrays [1], [2], [3], [4], [5]. Although III-V materials have good absorption coefficients for near-infrared (NIR) light, the devices still face the bottleneck of high material cost and incompatibility with CMOS integration. Meanwhile, Si-based CMOS devices have superior performance, their applications are limited because Si cannot absorb light in the short-infrared band for its low absorption coefficient. The Germanium-on-Silicon (Ge-on-Si) photodetector array can be a promising candidate as it can detect NIR light and is compatible with the Si-based CMOS process. Considering the future integration of NIR photodetectors, as well as foreseeable cost reductions, it is necessary to develop Si-based germanium (Ge) APD arrays using CMOS-compatible fabrication processes.

At present, small waveguide Ge photodetector (PD) arrays have been reported [6], [7], [8], [9], [10], but there is a common problem of high dark currents. With the increase of the number of Ge PDs array, the dark current increases significantly. Regarding Ge-on-Si APD array, it was first reported in 2019 [11]. Although the electric field in germanium is reduced through the design of the separate absorption-charge-multiplication (SACM) structure, the single APD device in the array still suffered excessive dark current in μA range near the breakdown voltage. However, this CMOS-compatible oriented Ge-on-Si-APD array opens a path for low-cost and yet highly integrated detector scheme for NIR imaging.

II. Device Design

The basic principle of the device is based on the design of the APD, and the device structure is an extension of this basis. We designed unique surface-illuminated cascaded three-electrode Ge-on-Si APD arrays with overall dimensions of 38 μm (width) $\times$ 294 μm (length) as illustrated in Fig. 1. Compared with the single three-electrode Ge-on-Si APD (See the top right corner of Fig. 1) reported previously [12], the Ge-on-Si APD array has the advantages of a larger detection area and higher sensitivity. We designed three electrodes and analyzed the effect of the voltage applied to Ge on the current per pixel. Our cascaded Ge-on-Si APD arrays can also potentially be used as a PMT [13], [14] by means of parallel electrodes, which can well reduce the problem of excessive dark current from large-area PMT. The cascaded Ge-on-Si APD array can control the current characteristics of the device by applying a voltage on the Ge electrode, thereby optimizing the device's performance. Higher responsivity can be obtained at a lower dark current. The specific structure is shown in

Manuscript received 10 December 2022; revised 25 December 2022; accepted 27 December 2022. Date of publication 29 December 2022; date of current version 27 January 2023. This work was supported in part by the National Key Research and Development Program of China under Grant 2022YFB2804504, in part by the National Natural Science Foundation of China under Grant 61934003 and Grant 62090054, in part by the Jilin Scientific and Technological Development Program under Grant 20200501007GX and Grant 20210301014GX, and in part by the Program for Jilin University (JLU) Science and Technology Innovative Research Team under Grant JLUSTIRT and Grant 2021TD-39. The review of this letter was arranged by Editor T.-Y. Seong. *(Corresponding author: JunFeng Song.)*

XiaoBin Liu, XueTong Li, YingZhi Li, ZiHao ZHi, BaiSong Chen, HeMing Hu, XueYan Li, FengLi Gao, and BoNan Kang are with the State Key Laboratory of Integrated Optoelectronics, College of Electronic Science and Engineering, Jilin University, Changchun 130012, China.

QiJie Xie and QuanXin Na are with the Peng Cheng Laboratory, Shenzhen 518000, China.

PengFei Guo and GuoQiang Lo are with the Advanced Micro Foundry Pte Ltd. (AMF), Singapore 117685.

JunFeng Song is with the State Key Laboratory of Integrated Optoelectronics, College of Electronic Science and Engineering, Jilin University, Changchun 130012, China, and also with the Peng Cheng Laboratory, Shenzhen 518000, China (e-mail: songjf@jlu.edu.cn).

Digital Object Identifier 10.1109/LED.2022.3233038

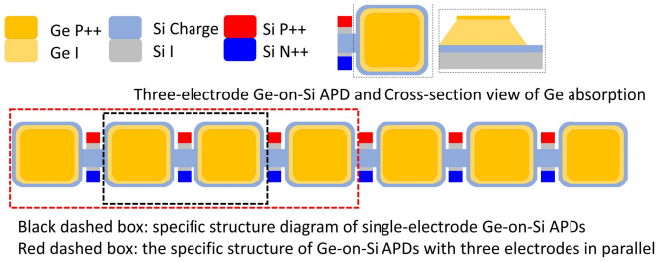

Fig. 1. Structure diagram of 1 × 7 Ge-on-Si APDs array interconnected by charge regions (Can be used as Ge-on-Si PMT). Three-electrode Ge-on-Si APD from a previous letter [12] is given in the upper right corner. The black and red dashed box gives the concrete structure of the two independent PMT.

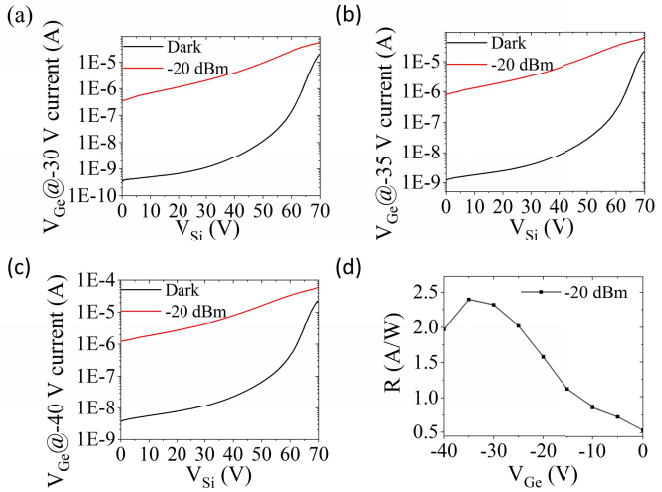

Fig. 2. Current characteristics of Ge-on-Si APDs (Two pixels). (a) −30 V on P++ Ge. (b) −35 V on P++ Ge. (c) −40 V on P++ Ge. (d) Responsivity at a dark current of 100nA at different applied Ge voltages.

Fig.1. In the array, one Si electrode can control two pixels. Although this cascaded device will have a certain amount of crosstalk, it can reduce the impact of pixel damage in the absorption area, which is more conducive to the measurement pulse time of the LiDAR.

III. Device Characterization

We first measured the current-voltage characteristics of a separate three-electrode APD. The specific test methods have been reported previously [12]. The current output characteristics of the device are controlled by applying different voltages on Ge (V_{Ge}). But unlike the previously reported single Ge-on-Si APD, the separate APD consists of two absorption regions (See the black dashed box in Fig. 1). The current characteristics under different V_{Ge} are shown in Fig. 2(a), (b) and (c). It is obvious that the photocurrent and dark current increase with the increase of V_{Ge}. The responsivity of the device at the low dark current level of 100 nA is analyzed. As shown in Fig. 2(d), when V_{Ge} is −35 V, the responsivity of the device is optimal at 2.4 A/W. The voltage is the optimal V_{Ge}, and its specific current characteristics are shown in Fig. 2(b). This shows that the device has better weak light detection ability; and compared with a single APD, it has two separated light absorption regions (2 pixels) with better sensing ability to divergent spatial light. Next, we use the

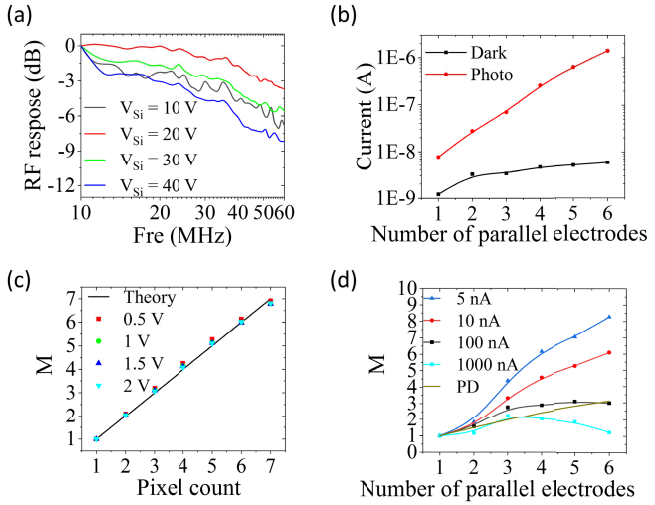

Fig. 3. (a) Normalized RF response characteristics of the Ge-on-Si APDs at −35 V on Ge. (b) Initial photo and dark current under different parallel electrodes. (c) Equally large Ge-on-Si PD normalized pixel photocurrent magnification. (d) Comparison of magnification of normalized amplified photocurrent at the same dark current level.

KEYSIGHT N4373D optical component analyzer to measure its radio frequency (RF) response characteristics. As shown in Fig. 3(a), the maximum 3dB bandwidth of the APD is 52 MHz (the corresponding optimal $V_{Ge} = -35$ V).

For better comparison, the PMT formed by seven Ge-on-Si APDs cascaded by interconnecting charge regions is different from a single APD. We designed new experiments to realize the overall current measurement of different large-area PMTs by changing the number of parallel electrodes. We tested the current characteristics of large-area Ge-on-Si PMTs with different pixel counts by using different numbers of parallel electrodes (The black dashed box and red dashed box in Fig. 1 represent the specific structure when the number of parallel electrodes is 1 and 3, respectively). The V_{Ge} maintains the optimal voltage of −35 V under different electrode number parallel connections. As shown in Fig. 3(b), we tested the initial photo-dark current under different parallel electrodes. We can find that the photo-dark current increases with the increase in the number of parallel electrodes. Especially when the number of parallel electrodes is 6 (7 pixels), the photocurrent is increased by about 180 times compared to a single electrode (2 pixels). At this time, the dark current is still within the nA level, which can improve the response of the device to weak light. Compared with our previously designed structure [12], the responsivity of the device at unity gain (at the punch-through voltage) is greatly improved.

To better demonstrate the advantages of the parallel electrode structure over the ordinary independent parallel devices. We introduced seven separate Ge-on-Si PDs as seven pixels (the same pixel size as our device). As shown in Fig. 3(c), A single pixel is normalized, and the overall current of multiple parallel pixels is compared to the current of a single pixel to calculate the magnification factor M. As the number of parallel electrodes increases, the number of pixels increases, resulting in an increase in photocurrent. And the increase factor M of the photocurrent is consistent with the number of parallel electrodes. This also confirms the principle of the parallel current increase in circuit theory. Since one parallel

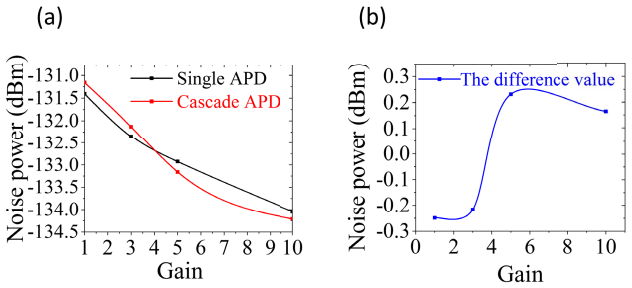

Fig. 4. (a) Excess noise comparison of a single device and a cascaded array device at different gains (with the same multiplication region width). (b) The magnitude of the excess noise difference between a single device and a cascaded array of devices.

electrode represents two pixels in our designed structure, we normalize the current represented by one parallel electrode in Fig. 3(d) and calculate the photocurrent magnification M of different numbers of parallel electrodes compared to one parallel electrode (The PD magnification M in the figure, in order to keep the area of the absorption area consistent, also normalizes the two pixels). We analyze the comparison of the magnification of our device and PD at the same dark current, see Fig. 3(d). We made our device have the same dark current under different numbers of parallel electrodes by changing the magnitude of the applied voltage to the device.

As shown in Fig. 3(d), When the dark current level is less than 100 nA, the PMT formed by the cascaded Ge-on-Si APD array has a larger magnification than the Ge-on-Si PD array. It is shown that the device performance of this structure is better than that of a simple parallel connected independent device structure under low dark current.

The cascaded Ge-on-Si APDs can achieve large-area low dark current Ge-on-Si APD fabrication. When the six parallel electrodes work together, the initial dark current is still at the nA level (Fig. 3(b)). When the dark current is fixed at 100 nA. The optical amplification factor of the six-electrode parallel is about three times that of the single-level (Fig. 3(d)). In theory, the overall responsivity of the device can reach more than 7 A/W at 100 nA (The best response of the single electrode is shown in Fig. 2(d)). This provides a new solution to reduce the dark current of large-area Ge-on-Si APDs, which are designed as PMTs in the form of cascaded APD structures. At the same time, the device can realize the array characteristics of Ge-on-Si APD through discrete electrodes, which has great potential in the field of weak light detection.

To better characterize the influence of excess noise on the device. We examined the excess noise of cascaded arrays and performed noise power tests for a single three-electrode APD and cascaded three-electrode APDs. We compared the noise of single devices and cascaded array devices with the same multiplication region in the case of the same gain, as shown in Fig. 4(a). The difference in excess noise between cascaded array devices and single three-electrode devices is about 0.25 dBm, as shown in Fig. 4(b). This shows that our cascaded device has a noise level comparable to a single three-electrode device. This is because the multiplication region of the device we designed has good independence, so as to ensure that the device will not cause a huge change in the excess noise due to the increase in the number of cascaded devices.

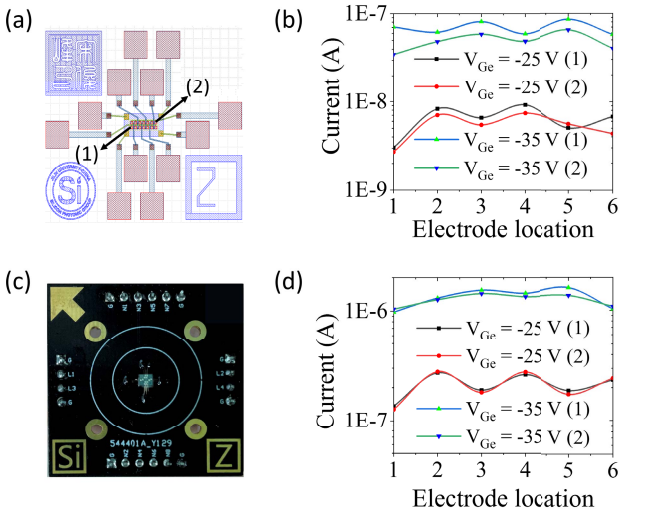

Fig. 5. (a) Ge-on-Si APD arrays (2 × 7) layout (Labels (1) and (2) are used to denote different two-row APDs). (b) Dark current of Ge-on-Si APD array under different V_{Ge}. (c) Packaged Ge-on-Si APD array chip. (d) Photocurrent of Ge-on-Si APD array under different V_{Ge}.

We packaged the chip and measured the spatial photocurrent properties of the cascaded Ge-on-Si APD (2 × 7) arrays, as shown in Fig. 5. We use the cascaded APD as six independent parts to test the current regulation characteristic of the three-electrode APD array, as shown in Fig. 5(b) and (d). A good demonstration of the feasibility of the current regulation of cascaded three-electrode APD arrays. Experiments show that the addition of different V_{Ge} can achieve the overall current regulation characteristics of the array. Using the independent characteristics of V_{Ge}, the output current can be adjusted by changing the size of V_{Ge} in NIR imaging to improve the accuracy of NIR imaging.

IV. Conclusion

Experiments show that the cascaded Ge-on-Si APD array has good weak light detection characteristics. The optimal responsivity of Ge-on-Si APD illuminated by a single electrode surface is as high as 2.4 A/W, which has a good detection effect on the spatially scattered weak light. When output as a single electrode independently, the overall current regulation of the array can be achieved through a unique structure. When used as a parallel overall structure, the PMT formed by the cascade structure can improve the weak light responsiveness of the device at the same dark current level. This low dark current CMOS process technology-compatible Ge-on-Si APD array points the way to low-cost, high-integration NIR 2D imaging detectors.

In the future, a vertical three-electrode structure can be considered. Avoiding the horizontal three-electrode design currently used, the separation between the avalanche region and the absorption region is defined by the ion implantation region. Due to process problems, the uniformity and repeatability of the ion-implanted area are poor. The avalanche region is manufactured by vertical epitaxy, which can precisely control the multiplication region's thickness, improve the device's uniformity, and obtain a higher multiplication rate. By forming an epitaxially extended charge layer array, the vertical structure can better improve the absorbing region's duty cycle and the device's bandwidth.

REFERENCES

[1] F. Ceccarelli, A. Gulinatti, I. Labanca, M. Ghioni, and I. Rech, "Red-enhanced photon detection module featuring a 32 × 1 single-photon avalanche diode array," *IEEE Photon. Technol. Lett.*, vol. 30, no. 6, pp. 557–560, Mar. 15, 2018, doi: 10.1109/LPT.2018.2804909.

[2] N. I. Iakovleva, K. O. Boltar, M. V. Sednev, A. I. Patrashin, and N. A. Irodov, "Short-wavelength infrared array avalanche photodetectors on the basis of InGaAs heteroepitaxial structures," *J. Commun. Technol. Electron.*, vol. 61, no. 3, pp. 319–323, Apr. 2016, doi: 10.1134/S1064226916030207.

[3] N. I. Iakovleva, K. O. Boltar, M. V. Sedneva, A. A. Lopukhin, and E. D. Korotaev, "320 × 256 avalanche array photodetector on the basis of ternary alloys of the A3B5 group with an InGaAs absorbing layer and an InAlAs barrier layer," *J. Commun. Technol. Electron.*, vol. 61, no. 3, pp. 348–351, Apr. 2016, doi: 10.1134/S1064226916030219.

[4] F. Nolet, N. Roy, S. Carrier, J. Bouchard, R. Fontaine, S. A. Charlebois, and J. F. Pratte, "22 μW, 5.1 ps LSB, 5.5 ps RMS jitter Vernier time-to-digital converter in CMOS 65 nm for single photon avalanche diode array," *Electron. Lett.*, vol. 56, no. 9, pp. 424–426, Apr. 2020, doi: 10.1049/el.2019.4105.

[5] S. Wang, H. Ye, L. Geng, Z. Lu, F. Xiao, F. Xiao, and Q. Han, "Design, fabrication, and characteristic analysis of 64 × 64 InGaAs/InP single-photon avalanche diode array," *J. Electron. Mater.*, vol. 51, no. 5, pp. 2692–2697, Mar. 2022, doi: 10.1007/s11664-022-09531-9.

[6] C. Chang, J. H. Sinsky, P. Dong, G. Valicourt, and Y. Chen, "High-power dual-fed traveling wave photodetector circuits in silicon photonics," *Opt. Exp.*, vol. 23, no. 7, pp. 22857–22866, 2015, doi: 10.1364/OE.23.022857.

[7] T.-C. Tzu, K. Sun, R. Costanzo, D. Ayoub, S. M. Bowers, and A. Beling, "Foundry-enabled high-power photodetectors for microwave photonics," *IEEE J. Sel. Topics Quantum Electron.*, vol. 25, no. 5, pp. 1–11, Sep. 2019, doi: 10.1109/JSTQE.2019.2911458.

[8] C. Xue, H. Xue, B. Cheng, W. Hu, Y. Yu, and Q. Wang, "1 × 4 Ge-on-SOI PIN photodetector array for parallel optical interconnects," *J. Lightw. Technol.*, vol. 27, no. 24, pp. 5687–5689, Dec. 15, 2009, doi: 10.1109/JLT.2009.2035090.

[9] D. Zhou, G. Chen, S. Fu, Y. Zuo, and Y. Yu, "Germanium photodetector with distributed absorption regions," *Opt. Exp.*, vol. 28, no. 14, pp. 19797–19807, Jul. 2020, doi: 10.1364/OE.390079.

[10] D. Zhou, Y. Yu, Y. Yu, and X. Zhang, "Parallel radio-frequency signal-processing unit based on mode multiplexed photonic integrated circuit," *Opt. Exp.*, vol. 26, no. 16, pp. 20544–20549, Jun. 2018, doi: 10.1364/OE.26.020544.

[11] Y. Li, X. Luo, G. Liang, and G.-Q. Lo, "Demonstration of Ge/Si avalanche photodetector arrays for LiDAR application," in *Proc. Opt. Fiber Commun. Conf. (OFC)*, 2019, p. TU3E.3.

[12] X. Liu, X. Li, Y. Li, Y. Li, Z. Zhi, M. Tao, B. Chen, L. Zhang, P. Guo, G.-Q. Lo, X. Li, F. Gao, B. Kang, and J. Song, "Three-terminal germanium-on-silicon avalanche photodiode with extended p-charge layer for dark current reduction," *Photon. Res.*, vol. 10, no. 8, pp. 1956–1963, Jun. 2022, doi: 10.1364/PRJ.452004.

[13] P. Buzhan, B. Dolgoshein, L. Filatov, A. Ilyin, V. Kaplin, A. Karakash, S. Klemin, R. Mirzoyan, A. N. Otte, E. Popova, V. Sosnovtsev, and M. Teshima, "Large area silicon photomultipliers: Performance and applications," *Nucl. Instrum. Methods Phys. Res. Sect. A, Accel., Spectrometers, Detectors Associated Equip.*, vol. 567, no. 1, pp. 78–82, Nov. 2006, doi: 10.1016/j.nima.2006.05.072.

[14] E. Leonora, S. Aiello, V. Giordano, N. Randazzo, D. L. Presti, D. Bonanno, F. Longhitano, and V. Sipala, "A study on large area Hamamatsu photomultipliers for Cherenkov neutrino detectors," *J. Instrum.*, vol. 10, no. 10, Nov. 2015, Art. no. T11003, doi: 10.1088/1748-0221/10/11/T11003.